

Supplementary Material: Data-Free Diversity-Based Ensemble Selection For One-Shot Federated Learning

1 Annotation of the main paper

- The value of K for Table. 3 in the main paper is 6.

2 Execution process of DeDES

Fig. 1 gives a flow chart of DeDES when we use the last layer of model parameters as the model representation and PCA as the dimension reduction method. The choice of clustering method will depend on the data partition which are shown in section 4.1.

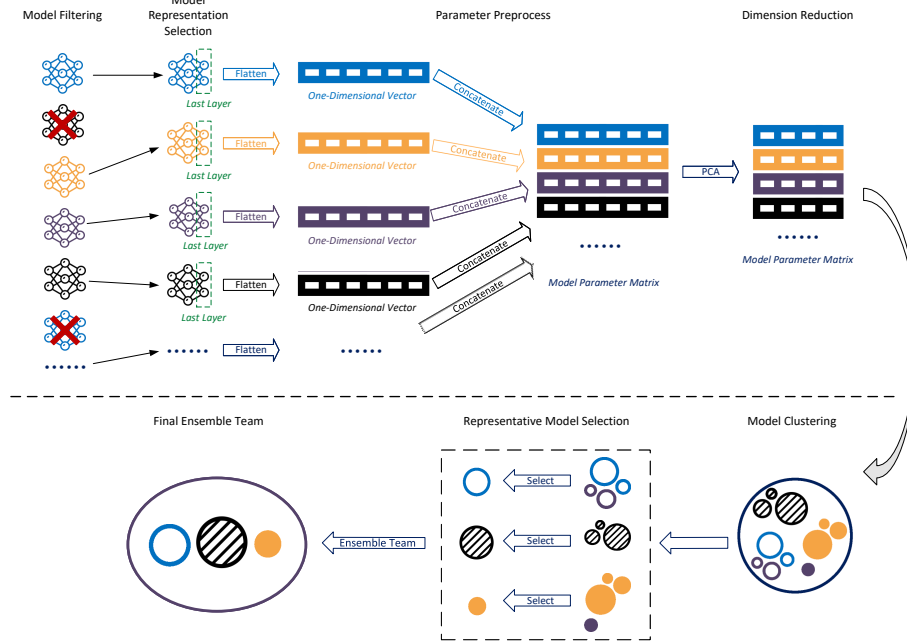


Fig. 1: Flow chart of the execution process of DeDES framework, where last layer is used to represent the model and PCA is used as the dimension reduction method.

Algorithm 1: `OutlierFilter` algorithm for the model filtering

Input: model set \mathcal{M} , truncated threshold pair (p_{low}, p_{high}) , interval scale s ,
and model scores $\mathcal{S} = \{s_i\}_{i=1}^m$.
Output: Outlier model set \mathcal{O} .
 \triangleright *Sort the score set \mathcal{S} , such as local validation accuracy, by ascending order.*
1 $\mathcal{S} \leftarrow \text{AscendingSort}(\mathcal{S})$
 \triangleright *Get the value of the p_{low} -th, p_{high} -th element of \mathcal{S} .*
2 $q_{low}, q_{high} \leftarrow \mathcal{S}_{p_{low}}, \mathcal{S}_{p_{high}}$
3 $interval \leftarrow q_{high} - q_{low}$
4 $outlier_threshold \leftarrow q_{low} - s * interval$
5 $\mathcal{O} \leftarrow \emptyset$
6 **for** $i = 1$ **to** m **do**
7 **if** $s_i < outlier_threshold$ **then**
8 $\mathcal{O} \leftarrow \mathcal{O} \cup \{M_i\}$
9 **return** \mathcal{O}

3 Model filter algorithm

As in Alg. 1 from the *main paper*, we use the `OutlierFilter` to obtain the outlier models \mathcal{O} based on the model scores \mathcal{S} provided from each party, which can be the local validation accuracy or prediction confidence. `OutlierFilter` can be any score-based unsupervised outlier detection methods; as we mentioned before, we utilized a variation of the commonly-used box-plot in our experiment, which is shown in the above Alg. 1.

As shown in Fig. 2, the 8-th party (i.e., p8) was not well-trained and not converge due to the inappropriate learning rate parameters, which results in an inferior validation accuracy (20.9%). Our method can successfully filter out this party’s model by the model filtering method when selecting ensemble teams, and can improve the final performance of ensemble learning.

4 Experiment Setup

4.1 Component Configurations

In this subsection, we will describe the default configurations of our `DeDES` framework for the experiments in the main paper.

For local model training, we utilize the *SGD* optimizer to train model for every party for 200 epochs with learning rate started at 0.1 and decrease at later epochs. After the training finished, we select the model with the highest local validation accuracy of each party to upload to the server of model market.

In our experiments, we select the final model layer as the model representation in our experiments; we utilize the *MINMAX* scaler to preprocess the *Model Representation Matrix*, and the *Gaussian Normalization* scaler to preprocess the

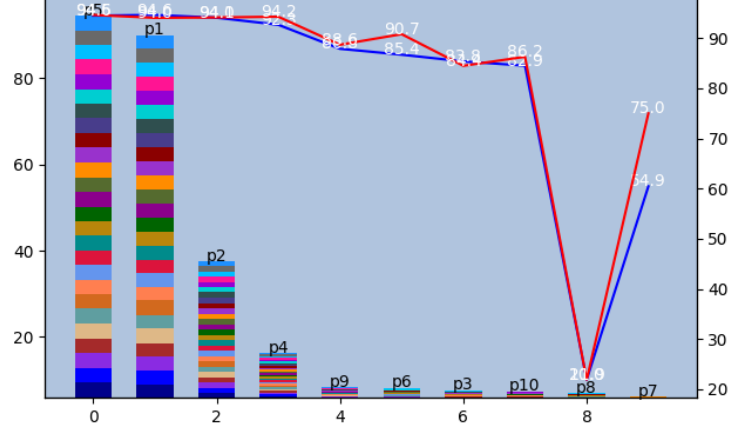


Fig. 2: Data distributions for the iid-dq partition of the EMNIST letters dataset with local validation accuracy and test accuracy for the whole test set when $m=10$. Every dot in the red line shows the best local validation accuracy after training for 200 epochs while the blue line shows the whole test accuracy of the k -th party p_k .

Label Distribution ground-truth input data; we do not utilize any dimension reduction strategies for the model representation matrix because the final layer of model parameters are already few in number.

Spectral clustering is used for the *homo* and *iid-dq* distribution partition methods; *K-Means* clustering is used for the *noniid-lds* and *noniid-lk* partition methods.

Our proposed model representative selection approach is utilized to determine the representative model within each cluster; as we have frequently stated, we use plurality voting to perform ensemble learning; we use the test accuracy as the evaluation metric for all the methods.

To compare the efficiency of different methods, we also recorded the running time of all methods, details will be shown in the experiment section. More details about the experimental settings, such as the devices we use or examples about four data partitions, are mentioned in the *supplementary material*.

4.2 Environment

All our experiments are running on a single machine with 1TB RAM and 256 cores AMD EPYC 7742 64-Core Processor @ 3.4GHz CPU. The GPU we used is NVIDIA A100 SXM4 with 40GB memory. The environment settings are: Python 3.9.12, PyTorch 1.12.1 with CUDA 11.6 on Ubuntu 20.04.4 LTS.

All the experimental results are the average over three trials.

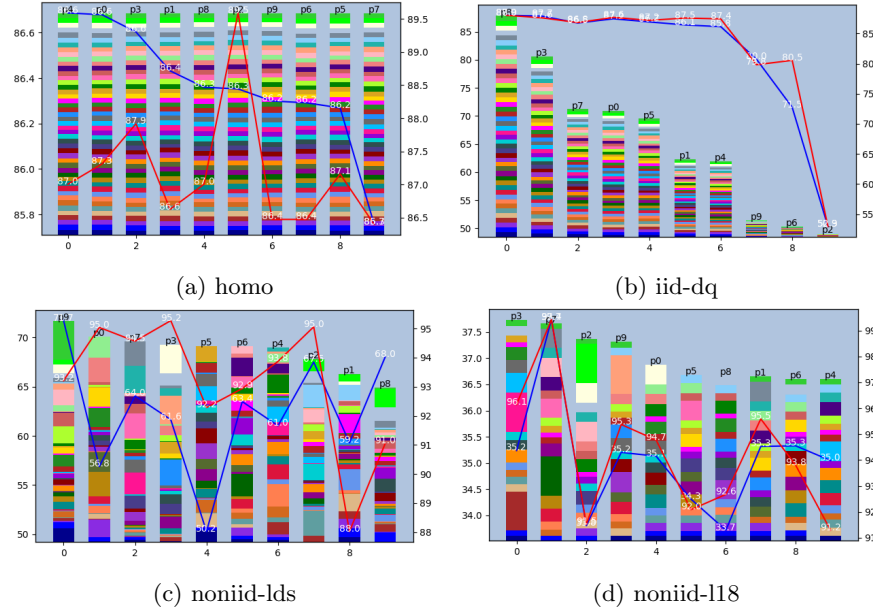


Fig. 3: Different data distributions of the EMNIST balanced dataset with local validation accuracy and test accuracy for the whole test set when $m=10$. Every dot in the red line shows the best local validation accuracy after training for 200 epochs while the blue line shows the whole test accuracy of the k -th party p_k .

5 Additional Experiments

In this section, we will show more experiment results as a supplement to the main paper. Due to the relatively large amount of experimental data, for each conclusion/finding, we take one of the experimental cases as presentation (one dataset, one m and one K), while the conclusion remains similar to other datasets/ m/K .

5.1 The importance of ensemble learning

Fig. 3 shows the data distributions of the EMNIST balanced dataset with local validation accuracy and test accuracy for the whole test set when $m=10$. We can see that the capacity of a single model is weak, even their local validation accuracy (validation accuracy for their own dataset) is high, therefore validates the importance of ensemble learning which can utilize the collaborative power of multiple models.

Table 1: Test accuracy (%) comparison for different dataset on different data partitions and model structures. The best and next best methods are **bolded** and underlined, respectively. If our DeDES method is better than the *LD* ground-truth method, the value of *LD* method will be marked in [skyblue](#).

Dataset	Partition	m	K	DeDES	AS	CV	DS	RS	FedAvg	MeanAvg	LD	Oracle
EMNIST Digits (Resnet-50)	homo	400	150	96.33	96.46	96.65	96.23	96.31	10.25	10.22	96.70	99.71
	iid-dq	400	150	98.13	98.01	98.08	98.07	97.94	10.63	10.64	98.13	99.70
	noniid-ld	400	150	96.52	<u>96.50</u>	86.58	95.48	96.04	10.24	10.19	94.80	99.70
	noniid-l3	400	150	<u>96.64</u>	96.81	89.21	58.59	94.72	9.74	9.61	96.83	99.67
EMNIST Letters (Resnet-50)	homo	200	120	<u>78.01</u>	77.91	78.77	77.13	77.08	3.86	3.89	77.41	94.76
	iid-dq	200	120	<u>88.88</u>	<u>88.88</u>	<u>88.88</u>	88.89	88.45	3.82	3.80	88.85	95.13
	noniid-ld	200	120	<u>79.78</u>	80.55	79.53	77.27	78.65	4.23	4.28	78.37	94.86
	noniid-l8	200	120	<u>81.10</u>	82.79	80.54	78.86	80.28	3.74	3.69	82.33	95.08
EMNIST Balanced (Resnet-50)	homo	100	50	<u>80.12</u>	80.11	80.33	79.38	79.20	2.15	2.18	78.93	89.44
	iid-dq	100	50	<u>85.68</u>	<u>85.68</u>	<u>85.68</u>	85.71	84.54	2.11	2.14	85.76	89.12
	noniid-ld	100	50	<u>76.34</u>	77.56	71.64	74.16	75.00	2.23	2.21	70.75	89.52
	noniid-l18	100	50	<u>77.99</u>	80.28	77.71	77.98	77.40	2.13	2.13	78.58	89.39
CIFAR10 (Densenet)	homo	200	100	46.84	46.30	<u>46.47</u>	45.37	45.68	10.49	10.08	46.34	90.57
	iid-dq	200	100	52.38	53.01	53.55	<u>53.47</u>	51.76	10.45	10.56	54.03	90.38
	noniid-ld	200	100	44.90	<u>43.91</u>	40.89	40.54	41.49	10.38	10.52	41.61	91.01
	noniid-l4	200	100	<u>47.04</u>	48.51	46.08	40.92	45.43	9.71	9.47	47.45	90.79
CIFAR100 (Deep Layer Aggregation)	homo	20	12	<u>23.01</u>	24.80	22.47	22.27	22.63	0.95	0.94	22.12	52.63
	iid-dq	20	12	<u>39.18</u>	39.18	<u>39.18</u>	<u>39.18</u>	37.04	1.01	0.95	39.18	55.61
	noniid-ld	20	12	<u>22.29</u>	25.11	21.37	21.88	21.15	0.94	0.94	21.42	55.94
	noniid-l45	20	12	<u>24.41</u>	27.42	24.07	23.08	23.59	0.87	0.85	23.19	54.90

5.2 Performance Analysis (Supplementary)

Table. 1 shows the performance of different methods when we apply them on the 5 datasets with 4 partitions with different model structures than the main paper. We can see that when $m = 200, K = 120$ for the EMNIST Letters Dataset, the test accuracy of DeDES and AS, CV are the same, which means they both selected the same ensemble teams.

Table 2 enumerated the accuracy of all 1024 teams and the ranking of selected teams generated by different methods for another data partition of the EMNIST balanced dataset. We can see that the ensemble team selected by DeDES is ranked higher than other baseline methods, which validates the efficacy of our method. Note the value of K here is 5 while the length of the best ensemble team for this dataset is 4, therefore, how to select an appropriate K remains an open problem.

5.3 Impact on Efficiency (Supplementary)

Fig.4 gives another plot of the relationship between K and test accuracy for the EMNIST Balanced dataset. The conclusion remains the same as the main paper that we don't have to select all models to form an ensemble team for most of the cases, which saves the inference time and also keeps good performance.

Method	Rank	Accuracy (%)
DeDES	214/1024	98.34
AS	372/1024	97.09
DS	608/1024	89.63
LD	675/1024	87.86
CV	933/1024	74.73
RS	952/1024	72.45

Table 2: Complete inspection on ensemble teams for *EMNIST Digits* dataset with $m = 10, K = 5$, *noniid-lds* partition.

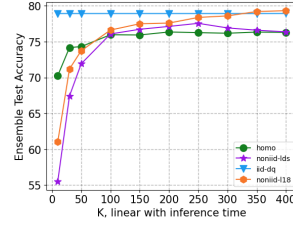


Fig. 4: The relationship of K and Ensemble Test Accuracy of DeDES for the *EMNIST Balanced* Dataset when $m=400$.

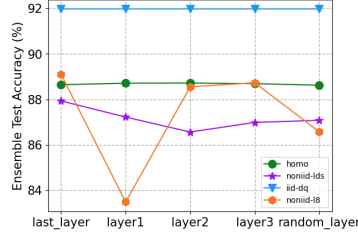


Fig. 5: The Ensemble Test Accuracy for different model representations of DeDES for the *EMNIST Letters* Dataset, VGG-5 (Spinal FC) structure when $m=200, K = 120$.

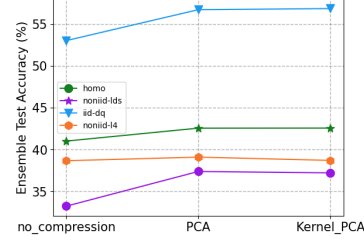


Fig. 6: The Ensemble Test Accuracy for different dimension reduction methods with the last layer model representation of DeDES for the *CIFAR10* Dataset, Resnet-50 structure when $m=50, K = 30$.

5.4 Ablation Studies

- **Performance Comparison on different model structures and datasets** Our method is solid for various model structures and datasets. As shown in Table 2. in the main paper and Table. 1 of this supplementary material, we can see that no matter what model structures/datasets we use, our method can achieve better performance than other baselines methods for ensemble learning.
- **Performance Comparison on different model representation** As shown in Fig. 5, for the VGG-5 (Spinal FC) model, layer1, layer2, layer3 and last_layer represent the first, middle, latter and final/last fully-connected layers of the model which are selected as the model representations and the random_layer means we randomly select 10 % of the layers as our model representation. As we can see, for the iid partitions (homo and iid-dq), the is almost no performance difference no matter what layer we choose; however, for the noniid partitions (noniid-lds and noniid-118), there is still a gap in the performance of different layers as representations. From the figure we can see that it is better to use the models' later layer's parameters for representation than utilizing their front layer's parameters as rep-

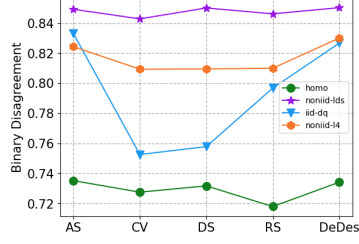


Fig. 7: The Binary Disagreement of different ensemble selection methods for the *CIFAR10* Dataset, Resnet-50 structure when $m=50$, $K = 30$.

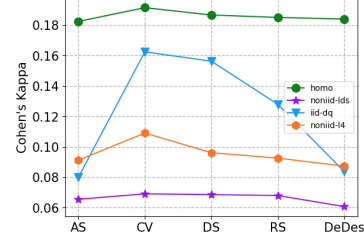


Fig. 8: The Cohen's Kappa for different ensemble selection methods of the *CIFAR10* Dataset, Resnet-50 structure when $m=50$, $K = 30$.

representations but it is just a crude conclusion that doesn't apply to all situations. Therefore, how to select a good model representation to get better performance remains an open problem and is important for the noniid data partition.

- **Importance of Dimension Reduction Methods.** As shown in Fig. 6, we compare three (dimension reduction) methods: PCA, Kernel_PCA and no_compression which means we don't compress the model representation, which is the last layer of the model. We reduced the model representation to m dimensions. We can see that generally, the *Kernel-PCA* is better than other dimension reduction methods such as *PCA* and *non-compression*. This is because the Kernel-PCA can convert non-linearly separable data to a new low-dimensional subspace suitable for alignment for linear classification, which is suitable for the deep learning models, which is non-linearly separable. Similar as the ablation study of model model representations, how to design a more effective dimension reduction method is still an open problem.
- **Clustering/Diversity validation** To validate our clustering results, we compare the Binary Disagreement (BD) [1] and the Cohen's Kappa (CK) [2] value of different methods to measure their diversities. The binary disagreement is defined as the ratio of the number of samples on which two models M_i and M_j get different prediction value to the total number of samples they predicted, higher binary disagreement means higher diversity; the cohen's kappa measures the agreement between two models in view of their reliability, lower cohen's kappa value indicates higher diversity (lower agreement). We take the average value of BD/CK for all pair (M_i, M_j) to get the final binary agreement/cohen's kappa value for the whole team \mathcal{M}_K^* .

As shown in Fig. 7 and Fig. 8, compared to other baseline methods, the ensemble team's diversity of **DeDES** is higher (higher BD or lower CK), which also means the agreement of the whole team's models are low. Since we select one model from every cluster, so this finding also indicates that our method can really cluster similar models together, which validates that **DeDES** can really generate an ensemble team with high diversity after clustering. Note that the All Selection (AS) method can also have high diversity compared to **DeDES** and meanwhile have high test ensemble accuracy, which validates the conclusion that the more diverse the models, the higher the ensemble's performance will have.

References

1. Ludmila I Kuncheva and Christopher J Whitaker. Measures of diversity in classifier ensembles and their relationship with the ensemble accuracy. *Machine learning*, 51(2):181–207, 2003.
2. Mary L McHugh. Interrater reliability: the kappa statistic. *Biochemia medica*, 22(3):276–282, 2012.